Annals of R.S.C.B., ISSN:1583-6258, Vol. 25, Issue 6, 2021, Pages. 3938 - 3952
Received 25 April 2021; Accepted 08 May 2021.

A Robust Noise Reduction Strategy in Magnetic Resonance Images

B. Ravi[1*], Vijendar Amgothu[3], Kumar Keshamoni[2,4], Anandeshi Vinisha[2], Praveen Kumar Poola[1*], Mohammad Obaidullah Khan[5]

[1]Associate Professor, Department of ECE, KLEF deemed to be University, Hyderabad-500030.
[2]Research Scholar, Department of ECE, KLEF deemed to be University, Hyderabad-500030.
[3]Associate Professor, CSE Department.Mallareddy Engineering College, Hyderabad-500100
[4]Assistant Professor, Vaagdevi Engineering College, Warangal-506002.
[5]Electrical Engineering Department, College of Engineering, Imam Mohammad Ibn Saud Islamic University, Riyadh, Saudi Arabia.

***Equal contribution**
Corresponding authors: raviou2015@klh.edu.in, prawinpoola@klh.edu.in

ABSTRACT

Magnetic Resonance imaging (MRI)is an indispensable tool and plays an important role in diagnosing the tumors in soft tissue. However, the added noise to the MRI scan during the acquisition will degrade the quality, which will result in fault/incorrect diagnosis of the disease.In order to address this challenge, time averaging concept was introduce to increase the signal noise ratio, but this concept will decrease the spatial resolution and increase the acquisition time, which in turnwill increase the patient exposure time to the radiation. Then the ray of hope was on computational methods and designing the algorithms. In this line many works were proposed. Here we are proposing a noise reduction schemeto estimate the noise from ground truth image. We mainly modelled the rician noise in this work.Then we considered modified Dual tree complex Wavelet Transform in the initial step followed by Rotational invariant version of Non-Local Mean filtering with the sparse matrix assumption. The proposed methods were evaluated using the performance metrics Peak signal-to-noise ratio (PSNR) and Image Structural Match Measure (ISMM).

Keywords: Wavelet Transform, Rician Noise, Non-Local Mean filter (NLM).

1. INTRODUCTION

Brain is a complex organ of human nervous system. A gigantic network in the brain is formed by billions of neurons[15][35][36][37]. Now a day's brain disorder is one of the major factors for causing death in individuals with different age groups. Pathological Brain Detection System (PBDS) have drawn more attention from researchers over past few years due to their significance in taking correct

Annals of R.S.C.B., ISSN:1583-6258, Vol. 25, Issue 6, 2021, Pages. 3938 - 3952
Received 25 April 2021; Accepted 08 May 2021.

medical diagnosis. Tumor is a mass of tissues which are caused due to uncontrollable and abnormal growth of cells in thebrain.A Multiple Sclerosis Lesion (MSL) and brain tumor are the common brain disorders can be detected using Magnetic Resonance Imaging (MRI)[35][36][37]. The MRI offers high resolution images of soft tissues than any other medical imaging modalities.Typically, MRI images contain blurring artifacts, motion artifacts, partial volume effects and Rician noise. Therefore, an accurate identification and detection of brain disorders in MRI images is very difficult in medical applications. The challenge lies in obtaining details of tumors/MSLsuchasthe location of tumor, size and shape from these brain MRI images.

The Rician noise and intensity in-homogeneities were added in MRI image while acquisition process is not considered by conventional image segmentation methods. The aim is to eliminateRician Noise, intensity in-homogeneitiesalong with segmenting the Multiple Sclerosis Lesion and tumor in brain MRI. A Multiple Sclerosis Lesion (MSL) and brain tumor are the common brain disorders that can be detected using Magnetic Resonance Imaging (MRI). The MRI offers high resolution images of soft tissues than any other medical imaging modalities. Typically, MRI images are plagued with artifacts such as blurring, partial volume effects, Rician noise and motion artifacts. Therefore, an accurate identification and detection of brain disorders in MRI images is very difficult. The challenge lies in obtaining details of tumors/MSL such as the location of tumor, size and shape from these brain MRI images. It is essential to remove these artifacts before applying the algorithms on MRI images for accurate feature extraction otherwise the obtained results might not be accurate as they are plagued with this noise.

MR Imaging (MRI) is commonly used Clinical imaging technique because it is noninvasive, high soft tissue contrast and high spatial resolution[35][36][37].. It is used for envisage the complete inner structure of the body in order to know pathological or other structural changes of any existing soft tissue. The frequency domain magnetic dipole movement characterization of tissue volume is obtained during MRI scanning [1], To convert this data in to spatial domain an inverse Fourier transform is applied which indicates the morphological and physiological characteristic features related to scanned patient. Thus, noise within the k- space (frequency domain) of MRI at each and every coil are considered mean as zero Gaussian function with same variance in real and imaginary part of the Fourier transform which is uncorrelated in nature [2]. In the past decade, there are many methods for noise reduction of MR images [3-4] have been proposed which includes the classic approaches like ADF [5-7], NDF [8] of magnetic resonance images through spatially changing noise ranges and adaptive noise

Annals of R.S.C.B., ISSN:1583-6258, Vol. 25, Issue 6, 2021, Pages. 3938 - 3952
Received 25 April 2021; Accepted 08 May 2021.

levels, the nonlocal means algorithm [9]. The rician noise is added while MRI acquisition process [10] which is needed to remove before further processing [11-15].

The remaining part of paper is organized: In section 2 a basic Noise model is presented, in Section 3 proposed algorithm is described in detail, Section 4 presents results and discussion and section V concluding remarks are presented.

2. NOISE MODEL

MR image artifacts are image noise, partial volume effect (PVE) and bias field effect. These artifacts will changes with different acquisition parameters, changes from one slice to another slice and changes from person to person under scanning. The Rician noise present in MR images not only disturbs the clinical decision and MR Image spatial quality [16-25].

The poison noise can be seen commonly in MRI images and satellite images The Poisson distribution with standard deviationμ is given by,

$$P_\mu(k) = \frac{e^{-\mu}\mu^k}{k!}, k \geq 0. \quad (1)$$

The $K = f(x)$, $f(x)$is an image need to recover. The de-noising equation using MAP estimator is based on Aubert and Ajol, 2008 [AA Model]. Applying Bayes law

$$P(f(x)|u) = P_{u(x)}\big(f(x)\big) = \frac{e^{-u(x)}u(x)^{f(x)}}{f(x)!} \quad (2)$$

Here assume that the region Ω is pixellated, and that the values of f at the pixels $\{x_i\}$ are independent. Then

$$P(f|u) = \prod_i \frac{e^{-u(x_i)}u(x_i)^{f(x_i)}}{f(x_i)!} \quad (3)$$

The value of $p(u)$is from total variation (TV) regularization model,

$$P(u) = e^{-\beta} \quad (4)$$

Where Ω denotes the image domain, from the AA model which can minimize $-log(p(f|u)p(u))$. By applying Log on equation (3.1) and simplifying,

$$E(u) := +\beta \quad (5)$$

Annals of R.S.C.B., ISSN:1583-6258, Vol. 25, Issue 6, 2021, Pages. 3938 - 3952
Received 25 April 2021; Accepted 08 May 2021.

The $E(u)$ can be minimized using Euler-Lagrange equation and discretized Partial Difference Equation (PDE) i.e

$$u_t = div\left(\frac{\nabla u}{|\nabla u|}\right) + \frac{1}{\beta u}(f - u) \qquad (6)$$

Where as f denotes the observed image u_0, div is divergence operator.

The presence of this noise is problematic and challenging for further image processing operations like region of interest finding, any organ segmentation, Image Classification, image registration and image reconstruction etc. The MR image $y(i,j)$ is liner combination of noise free image and additive noise $n(i,j)$ i.e

$$y(i,j) = x(i,j) + n(i,j) \qquad (7)$$

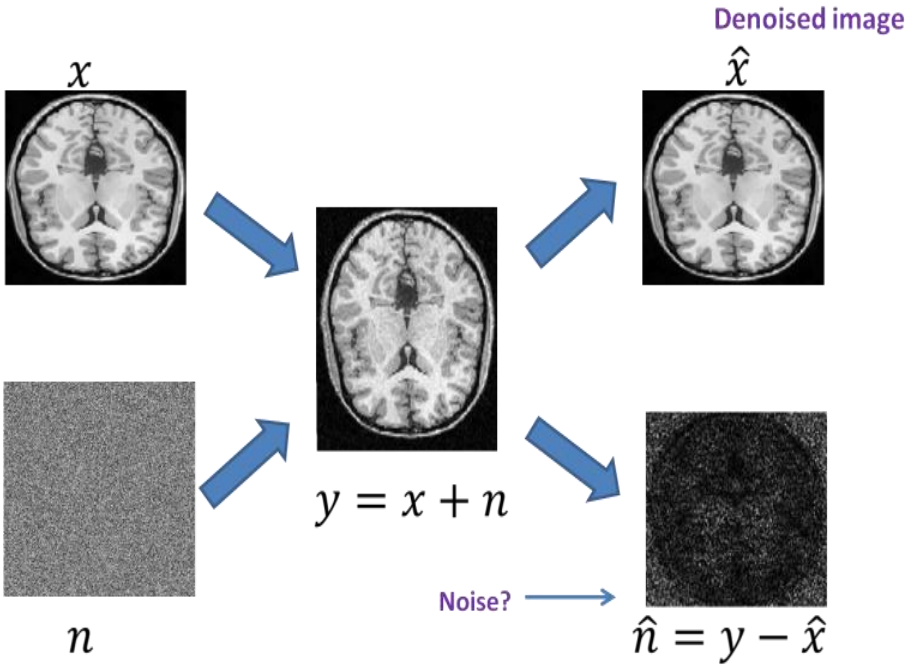

Figure 1 Noise Model

3. PROPOSED METHOD

The aim of noise reduction processes is to discover good estimation of $x(i,j)$, from $y(i,j)$. In the above figure the y is image with noise, $\hat{x}$ is the estimation/ de-noised image and $\hat{n}$ noise residue.

Annals of R.S.C.B., ISSN:1583-6258, Vol. 25, Issue 6, 2021, Pages. 3938 - 3952
Received 25 April 2021; Accepted 08 May 2021.

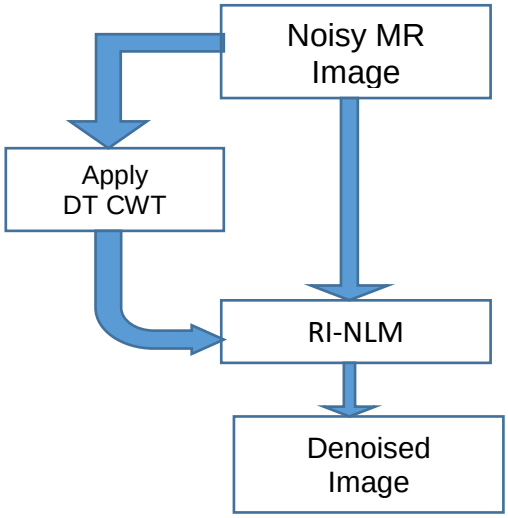

Figure 2 Proposed Block Diagram

This is done by Dual Tree based Complex Wavelet Transform for noise reduction that uses sparseness of image and Rotational invariant version of Non-Local Mean filter.

3.1.Dual Tree Complex Wavelet Transform (DT-CWT)

The normal DWT, the slight change with the input image or signal can effect substantial variations in the dissemination of 2D signal/1D signal energy through different scales with in coefficients values of DWT that is shift variant, lack of directional orientation and aliasing. N. Kingsbury (N. Kingsbury, 1999) presented a novel category of wavelets for image processing, which is known as the Dual Tree based Complex Wavelets. To solve/overcome the problems of orthogonal decrease wavelets, we have chosen the dual tree CWT, which is having dual tree filters with real coefficients and imaginary. The coefficients are approximately shift invariant in terms of amplitude, the directional selectivity in 2D is having around six orientations and redundancy is very limited (i.e sparse in nature), redundancy is independent of decomposition order.The one dimensional Dual Tree-CWT sub divides the given signal via expanding it with complex shifted then dilated root wavelet $\varphi(x)$and scaling factor $\emptyset(x)$, i.e.,

$$f(x) = \sum_{l\in Z} S_{j_{0,}l}\emptyset_{j_{0,l}}(x) + \sum_{j\geq j0}\sum_{l\in Z}\varphi_{j,l}(x) \quad (8)$$

The 2-D Dual Tree-CWT sub-divides a two dimensional signal/ image f(x, y) with a periodic translations and dilations of a complex scaling factor, which is represented as

$$f(x,y) = \sum_{l\in Z^2} S_{j0,l}\,\emptyset_{j0,l}(x,y) + \sum_{\theta\epsilon\,\Theta}\sum_{j\geq j_0}\sum_{l\in Z^2} C_{j,l}^{\theta}\varphi_{j,l}^{\theta}(x,y) \quad (9)$$

Annals of R.S.C.B., ISSN:1583-6258, Vol. 25, Issue 6, 2021, Pages. 3938 - 3952
Received 25 April 2021; Accepted 08 May 2021.

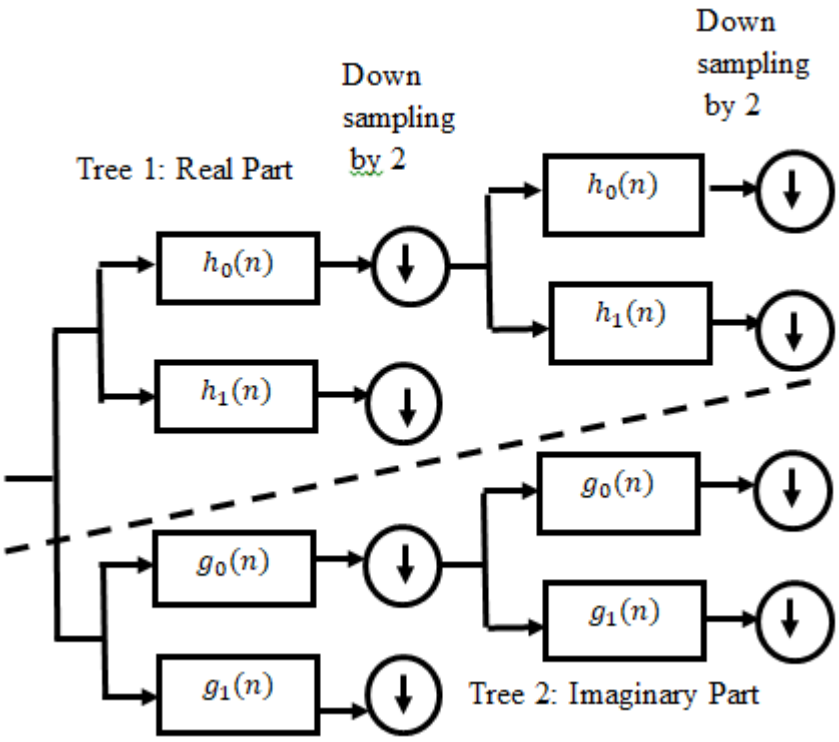

Figure 3 Block Representation of DT-CWT

Where $\theta \epsilon \Theta = \{\pm 15^o, \pm 45^o, \pm 75^o\}$ indicates the directionality related to complex wavelets. The Dual Tree-CWT results in one LP sub-band and six HP sub-bands which are complex at every stage of subdivision, where every HP sub-band related to one new direction. The noise reduction is performed first using Dual Tree CWT then it is given to RI-NLM filter. The similarity between pixels and patches are computed with RI-NLM Filter, the obtained output is having better Peak Signal to Noise Ratio (PSNR) and Better Image structural match Measure (ISMM) [26-34].

3.2.Non Local Means (NLM) filter

The NLM de-noising algorithm was first applied by replacing a pixel with the related neighborhood pixels (Manjon JV. et al, 2010). The algorithm is generalized through a patch adjusted analysis at every pixel instead of pixel itself. The NL Mean algorithm works based on weighted mean of the adjoining mask spots, whereas this algorithm is extremely governed with the patch similarity among neighboring pixels.

Thus by considering the ordinary NLM (Thacker NA, 2010).) With pixel by pixel process is time consuming. So instead of this search windows are considered for decreasing the processing time. The noise reduction process is repetitive in nature in terms of pixel by pixel, it is represented as

Annals of R.S.C.B., ISSN:1583-6258, Vol. 25, Issue 6, 2021, Pages. 3938 - 3952
Received 25 April 2021; Accepted 08 May 2021.

$$NLM(X_i) = \sum_{X_j \in SW} w(X_i, X_j).\mu(X_j) \quad (10)$$

Here $X_i and\ X_j$ ware specific measures of image intensity on particular pixels i in addition to j. X_j is related with searching window mask which is related to adjacent pixels. μRepresents specific pixel intensity of image $X.w(X_i, X_j)$ Denotes the weight function for the pixels i and j, this weight function represents the difference between pixel i and j.

$$w(X_i, X_j) = \frac{1}{C(X)} \sum_{\delta \epsilon P} e^{-\frac{G_a \left|\mu(X_i+\delta)-\mu(X_j+\delta)\right|^2}{h^2}}$$

In the above equation $G_a$represents the gaussian kernel

$$\hat{x}(i) = \frac{\sum_{j=\Omega} \beta(i,j) y(i)}{\sum_{j=\Omega} \beta(i,j)}$$

$$\beta(i,j) = e^{-\frac{1}{2}\left(\frac{\left(\hat{x}^0(i)-\hat{x}^0(j)\right)^2+3\left(\mu^0_{N_i}-\mu^0_{N_j}\right)^2}{2h^2}\right)}$$

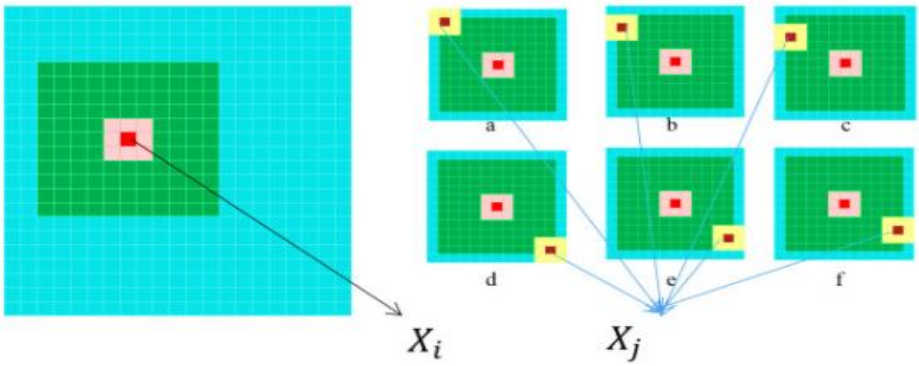

Figure 4. NL means Patch based Similarity measurement Processes

The patches which are having an intensity variance more than h does not leads to the noise reduction process. This process is called rotational invariant NLM (PRI-NLM). Since the projected similarity measure was given to an already noise reduced image with the Dual Tree-CWT algorithm, the constraint h controls the filtering capability of the NLM filter. This proposed algorithm is showing extremely good performance with different types of images and at various level of noisy conditions.

The performance of noise reduction method is measured with the help of "PSNR" and Structural Similarity Index Method (SSIM). For an image $I_1(i,j)$ and $I_2(i,j)$ PSNR is

Annals of R.S.C.B., ISSN:1583-6258, Vol. 25, Issue 6, 2021, Pages. 3938 - 3952
Received 25 April 2021; Accepted 08 May 2021.

calculated as follows

$$MSE = \frac{\sum_{I,J}[I_1(i,j) - I_2(i,j)]^2}{I * J} \quad (11)$$

$$PSNR = 10\log_{10}\left(\frac{R^2}{MSE}\right) \quad (12)$$

Where $I_1(i,j)$ is original image, $I_2(i,j)$ is denoised image and R is the maximum gray scale value of image. Structural similarity index term is computed with the help of three parameters luminance(l), the contrast(c), and the structural(s) components of an image

$$SSIM(i,j) = [l(i,j)]^{\alpha}[c(i,j)]^{\beta}[s(i,j)]^{\gamma} \quad (13)$$

In the equation (3.9) $l(i,j)$, $c(i,j)$ and $s(i,j)$ are calculated with help of $\mu_{i,}\mu_j, \sigma_i\sigma_j \; and \; \sigma_{ij}$: which are local means, standard deviation and cross-covariance of MR images.

$$l(i,j) = \frac{2\mu_i\mu_j + C_1}{\mu_i^2 + \mu_j^2 + C_1}$$

$$c(i,j) = \frac{2\sigma_i\sigma_j + C_2}{\sigma_i^2 + \sigma_j^2 + C_2}$$

$$s(i,j) = \frac{\sigma_{ij} + C_3}{\sigma_i\sigma_j + C_3}$$

In SSIM equation $\alpha = \beta = \gamma = 1$ these are default for exponents, and $C_3 = C_2/2$ (default selection of C_3) then the Structural Similarity Index simplifies as

$$SSIM = \frac{(2\mu_i\mu_j + C_1)(2\sigma_{ij} + C_2)}{(\mu_i^2 + \mu_j^2 + C_1)(\sigma_i^2 + \sigma_j^2 + C_2)} \quad (14)$$

In the table1 Proton Density- Weighted MRI of Brain is corrupted by Racine noise with 7%, T2- Weighted MRI of Brain degraded by 9% noise and T1- Weighted brain MRI degraded by 15%.

Brainweb web page provides Simulated Brain Magnetic Resonance Image Database (SBMRID). The SBMRID contains a large of realistic MR Image database with different volumes generated by an MRI simulator. This database will be used by the medical imaging research community to compare and evaluate the results of various MR image analysis algorithms.

Annals of R.S.C.B., ISSN:1583-6258, Vol. 25, Issue 6, 2021, Pages. 3938 - 3952
Received 25 April 2021; Accepted 08 May 2021.

Currently, the SBMRID consist of simulated brain MR Image database which depends on two anatomical formats: normal MR Image and multiple sclerosis (MS) MR image. For these two types of images, total 3-D volumes have been generated with help of three sequences T1, T2, and proton-density (PD) weighted.

The MR image is available at different slice thickness (1mm to 9mm), Ricin noise levels (0% to 9%), and levels of Intensity inhomogeneity (0% to 40%). The data visualization is possible in axial plane, sagittal plane, and coronal plane. The brain MR image data with different combination can be downloadable for further analysis. A user can also request for any new combination of slice thickness, noise level. The Table 3.1 Shows the results obtained using proposed method, this method is applied on PD-Weighted MRI, T2-weighted MRI and T1- weighted MRI images with 7% Rician noise.

4. RESULTS AND DISCUSSION

The simulation and implementation of Racine Noise Reduction using Dual Tree-Complex Wavelet Transform and Self similarity was done with Matlab2019a on a Windows Desktop Machine, i5, 4GB RAM, and Datasets Proton Diffusion (PD)-Weighted MRI, T2-Imaging MRI and T1- Imaging MRI are taken from Brainweb(C.A. Cocosco et al. 1997): simulated volumes for these three imaging modality are available online (T1, T2, PD), each modalities available with different measurement of slice wideness, noise and non-uniform image intensity .

The noise reduction is done using two stage processes, first Dual Tree-CWT applied, which will permits for dissimilarity of data orientation in the transform domain. The rotational invariant kind of Non-Local Mean filter is applied: similar patches will gain high weight as compared to the dissimilar patches.

Table 1 Result Comparison of Noise Reduction Methods

MR Image	De-Noising Methods	Performance Metrics	
		PSNR (dB)	SSIM
PD-Weighted MRI	ADF	25.37	0.9642
	NLML	26.52	0.9694
	NS Median	27.19	0.9787
	Proposed Method	32.30	0.991
T2-Weighted MRI	ADF	22.67	0.9466

Annals of R.S.C.B., ISSN:1583-6258, Vol. 25, Issue 6, 2021, Pages. 3938 - 3952
Received 25 April 2021; Accepted 08 May 2021.

	NLML	23.75	0.9512
	NS Median	24.4	0.9696
	Proposed Method	28.24	0.9716
T1- Weighted MRI	ADF	16.84	0.8127
	NLML	18.96	0.8426
	NS Median	20.51	0.9062
	Proposed Method	22.42	0.934

In the above table1 Proton Density- Weighted MRI of Brain is corrupted by Racine noise with 7%, T2-Weighted MRI of Brain degraded by 9% noise and T1- Weighted brain MRI degraded by 15%.

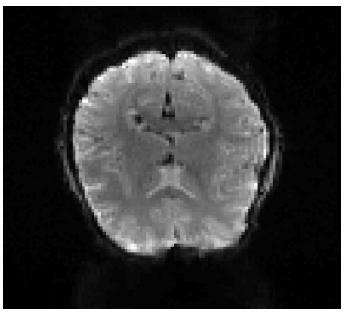

(i)

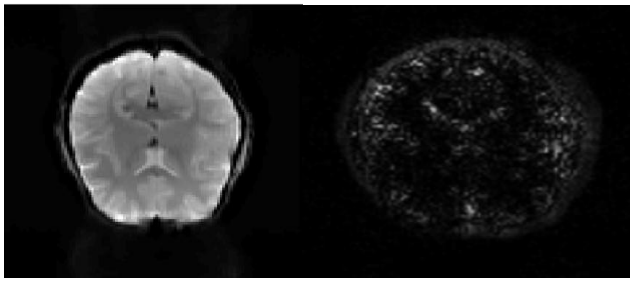

(ii) (iii)

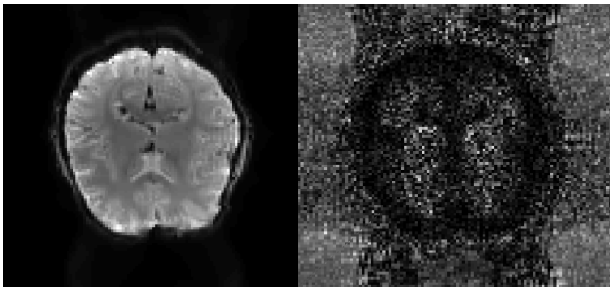

(iv) (v)

Annals of R.S.C.B., ISSN:1583-6258, Vol. 25, Issue 6, 2021, Pages. 3938 - 3952
Received 25 April 2021; Accepted 08 May 2021.

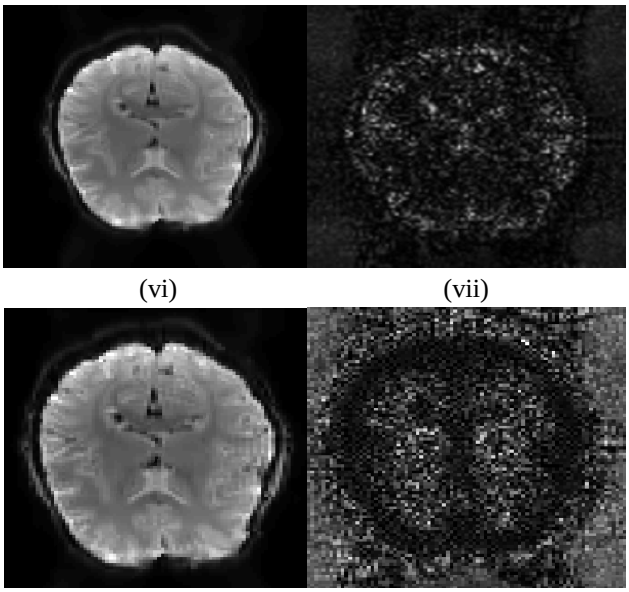

(vi) (vii)

(viii) (ix)

Figure 4 (i) Input Noisy data (ii) Denoised Output using ADF method (iii) Noise Residue using ADF (iv) Denoised Output using NLML method (v) Noise Residue using NLML, (vi) Denoised Output using NS method (vii) Noise Residue using NS method (viii) Proposed method Denoised output(ix) Proposed method Noise Residue

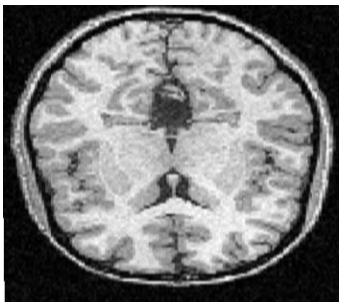

(i)

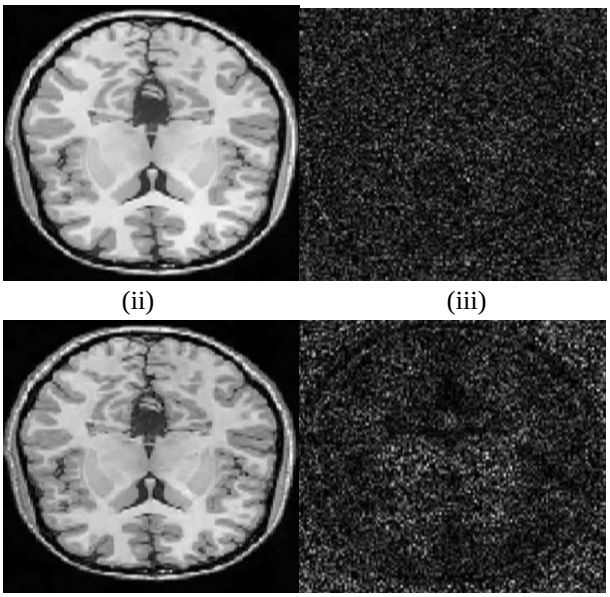

(ii) (iii)

(iv) (v)

Annals of R.S.C.B., ISSN:1583-6258, Vol. 25, Issue 6, 2021, Pages. 3938 - 3952
Received 25 April 2021; Accepted 08 May 2021.

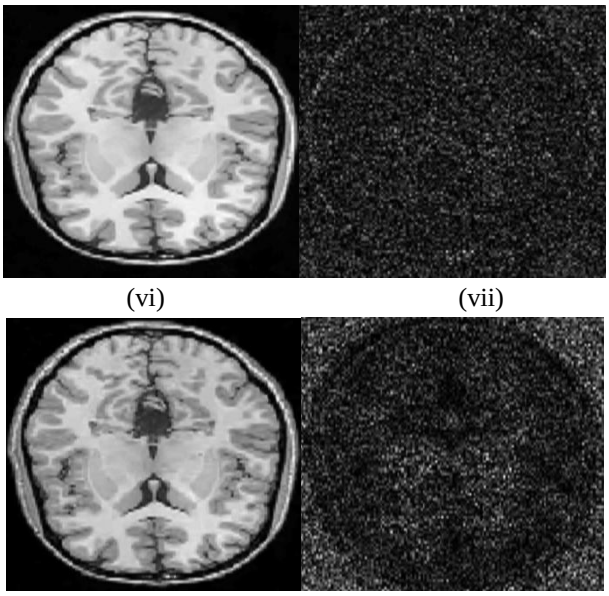

(vi) (vii)

(viii) (ix)

Figure 5 (a) Input Noisy data (b) Denoised Output using ADF method (c) Noise Residue using ADF (d) Denoised Output using NLML method (e) Noise Residue using NLML, (f) Denoised Output using NS method (g) Noise Residue using NS method (h) Proposed method Denoised output(ix) Proposed method Noise Residue

Noise Level (%)	**0**	**3**	**6**	**9**	**12**	**15**
ADF[74]	28	27.5	25	22.5	20	18
NLML[74]	38	33	26.5	22.5	22	19
NS Median[74]	38.5	34	27.5	24	22.5	20
Proposed Method	39.5	35	28	24	23	21.5

Table 2 PSNR Simulation results of T1 weighted MRI with various Noise levels

The table 2 shows the PSNR obtained at different Rician noise levels 0% to 15% in steps of 3%. From the obtained results the PSNR is decreasing as Rician noise level increases. The Rician noise reduction methods, Anisotropic Diffusion Filter (ADF), Non local Maximum Likelihood (NLML), Nutrosophic Set Median Filter (NS median) and Proposed DT-CWT

Annals of R.S.C.B., ISSN:1583-6258, Vol. 25, Issue 6, 2021, Pages. 3938 - 3952
Received 25 April 2021; Accepted 08 May 2021.

based RI-NLM were compared with PSNR value, the proposed method has superior PSNR at all levels of Rician noise.

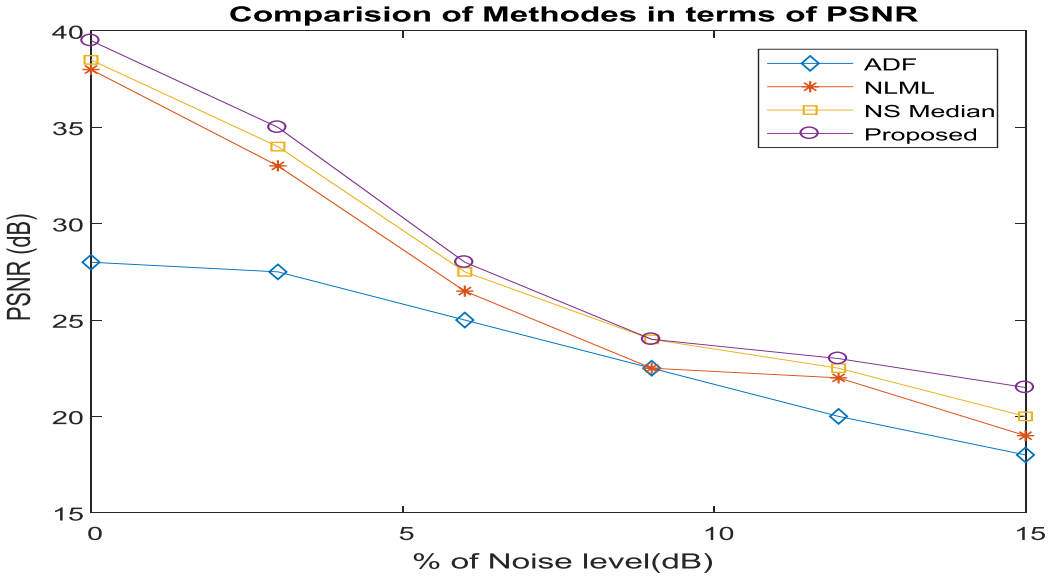

Figure 6 PSNR obtained by different Noise Reduction Methods

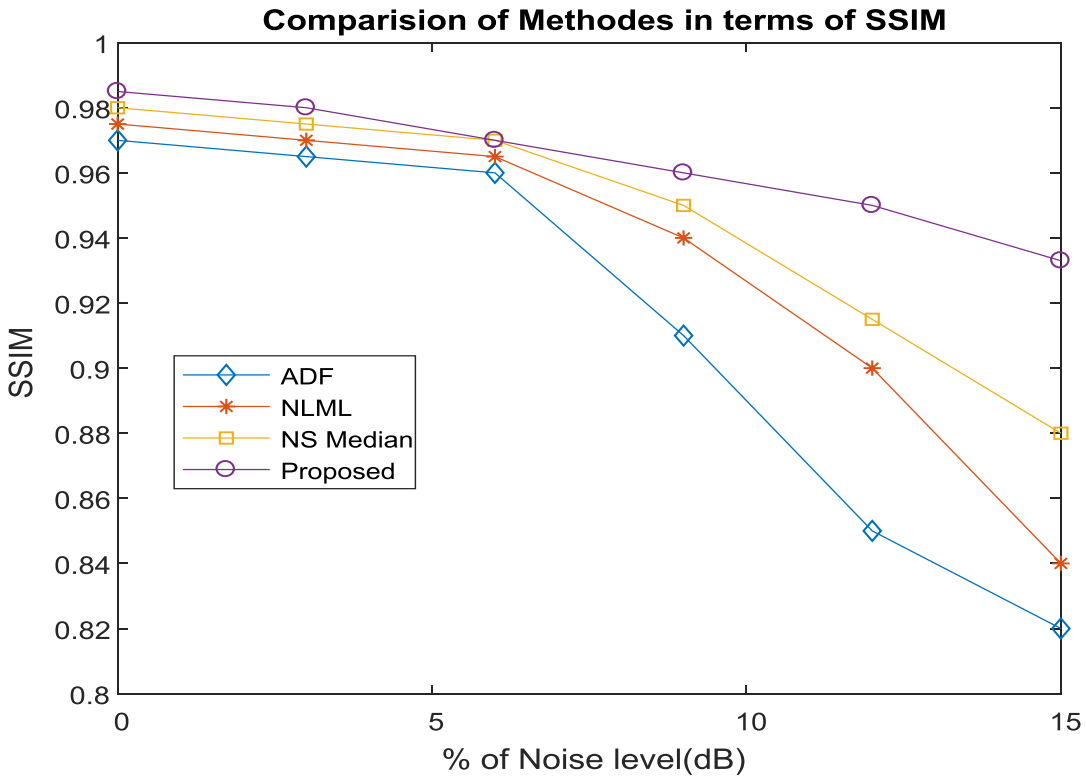

Figure 7 SSIM obtained by different Noise Reduction Methods

5. CONCLUSION

The proposed algorithm is based on Dual Tree-CWT and Nonlocal Mean Filtering processes are used to

Annals of R.S.C.B., ISSN:1583-6258, Vol. 25, Issue 6, 2021, Pages. 3938 - 3952
Received 25 April 2021; Accepted 08 May 2021.

eliminate Rician noise from the brain magnetic resonance images. The noise reduction is done using two stage processes, first sparse DT-CWT is applied, which allows for distinction of data directionality in the transform space and then Rotational invariant version of Non-Local Mean filter is applied. The proposed algorithm is tested with different Rician noise levels of brain MR Images. Even the Image is degraded by 15% Rician noise the PSNR and SSIM obtained are 23dB and 0.93 which is a better performance as compared to conventional methods.

6. REFERENCES

1. G Saranya, SN Devi "An Approach for Spread Spectrum based Data Embedding and Retrieving using Optimization Technique in Medical Image" *International Journal of Imaging and Robotics*, 2018.
2. N. Kingsbury, "Image processing with complex wavelets," *Philos. Trans. R. Soc. London A, Math. Phys. Sci.*, vol. 357, no. 1760, pp. 2543–2560, Sep. 1999.
3. J.Mohana, V.Krishnaveni, YanhuiGuoc, "MRI denoising using nonlocal neutrosophic set approach of Wiener filtering" Biomedical Signal Processing and Control Volume 8, Issue 6, November 2013, Pages 779-791
4. A. Buades, B. Coll, J.M. Morel, "*A review of image denoising algorithms, with a new one,MultiscaleModelingSimulation"*, 4 (2005)490-530.
5. Karl Krissian and Santiago Aja-Fernández "Noise-Driven Anisotropic Diffusion Filtering of MRI" *IEEETransactions on Image Processing, VOL. 18, NO. 10,* OCTOBER, 2009.
6. A. Samsonov, C. Johnson, *"Noise-adaptive nonlinear diffusion filtering of MR images with spatially varying noise levels, Magn*". Reson. Med.52 (2004) 798–806.
7. P. Perona, J. Malik, *"Scale-space and edge detection using anisotropic diffusion"*, IEEE Trans. Pattern Anal. Machine Intell. 12 (1990) 629–639.
8. R. Rodríguez, E. Torres, J. H. Sossa, Y. Garcés, "A new stopping criterion for the mean shift iterative algorithm. Its use in image segmentation" *International Journal of Imaging and Robotics*Volume 17, Issue Number 2, 2017.
9. PravinKshirsagar and SudhirAkojwar (2017), "Classification of ECG-signals using Artificial Neural Networks", Researchgate.net
10. S. Aja-Fernández, C. Alberola-López, C.F. Westin, Noise and signal estimation in magnitude MRI and Rician distributed images: A LMMSE approach, IEEE Trans. Image Proccessing,17 (2008) 1383–1398.
11. Ahammad, S.H., Rajesh, V., Neetha, A., SaiJeesmitha, B. &Srkanth, A. 2019, "Automatic segmentation of spinal cord diffusion MR images for disease location finding", Indonesian Journal of Electrical Engineering and Computer Science, vol. 15, no.3, pp.1313-1321.
12. Ahammad, S.H., Rajesh, V., Saikumar, K., Jalakam, S. & Kumar, G.N.S. 2019, "Statistical analysis of spinal cord injury severity detection on high dimensional MRI data", International Journal of Electrical and Computer Engineering, vol. 9, no.5, pp. 345-3464.
13. Ahammad, S.K.H., Rajesh, V. & Ur Rahman, M.Z. 2019, "Fast and Accurate Extraction-Based Segmentation Framework for Spinal Cord Injury Severity Classification", IEEE Access, vol.7, pp. 46092-46103.
14. Ahilan, A., Manogaran, G., Raja, C., Kadry, S., Kumar, S.N., Agees Kumar, C., Jarin, T., Krishnamoorthy, S., Malarvizhi Kumar, P., Chandra Babu, G., SenthilMurugan, N. &Parthasarathy 2019, "Segmentation by fractional order Darwinian Particle Swarm Optimization Based multilevel Thresholding and improved lossless prediction based compression algorithm for medical images", IEEE Access, vol.7, pp. 89570-89580.
15. Babu, K.R., Naganjaneyulu, P.V. & Prasad, K.S. 2019, "Performance analysis of fusion based brain tumor detection using Chan-Vese and level set segmentation algorithms", International Journal of Recent Technology and Engineering, vol.7, no.6, pp. 2089-2096.
16. Chakraborty, K., De, A. & Sharma, S.K. 2019, "Random walk segmentation algorithm for MRI of brain", Journal of Advanced Research in dynamical and control systems, vol. 1, no.4, pp.830-835.
17. Changala, R. &Rajeshwararao, D. 2019, "Development of predictive model for medical domains to predict chronic diseases (diabetes) using machne learning algorithms and classification technique", ARPN Journal of Engineering and Applied Sciences, vol. 14, no.6, pp.1202-1212.

18. Hariram, L., Kota, K., Vedha, J. &Bharathwaj, K. 2019, "Automated hippocampus segmentation", International Journal of Recent Technology and Engineering, vol.7, no.6, pp. 626-630.
19. HasaneAhammad, S., Rajesh, v. Hanumatsai, N., Venumadhav, A., Sasank, N.S.S., Bhargav Gupta, K.K. &Inithiyaz, S. 2019, "MRI image training and finding acute spine injury with the help of hemorrhagic and non hemorrhagic rope wounds method" , Indian journal of public health research and development, vol. 10, no.7, pp.404-408.
20. HemasundaraRao, C., Naganjaneyulu, P.V. &Satyaprasad, K. 2019, "Automatic classification breast masses in mammograms using fusion technique and FLDA analysis", International Journal of Innovative Technology and Exploring Engineering, vol.8, no.5, pp.1061-1071.
21. Jyoti Patil, M.S. &Pradeepini, G. 2019, "Development of deep learning algorithm for brain tumor segmentation", International Journal of Engineering and Advanced Technology, vol.9, no.1, pp.2800-2803.
22. K, R. &vinothkanna, R. 2019, "Hybrid ant colony optimization model for image retrieval using scale-invaraint feature transform local descriptor", Computers and Electrical Engineering, vol. 74, pp.281-291.
23. Poola, P.K., Kumaresan, Y., Krasnikov, I. and Seteikin, A., 2020. Terahertz Molecular Imaging and Its Clinical Applications. In Terahertz Biomedical and Healthcare Technologies (pp. 195-213). Elsevier.
24. Poola, P. K., Krasnikov, I., &Seteikin, A. (2020). Waveguides for Terahertz Endoscopy. In *Terahertz Biomedical and Healthcare Technologies* (pp. 215-224). Elsevier.
25. Poola, P.K. and John, R., 2017. Label-free nanoscale characterization of red blood cell structure and dynamics using single-shot transport of intensity equation. Journal of Biomedical Optics, 22(10), p.106001.
26. Poola, P.K., Afzal, M.I., Yoo, Y., Kim, K.H. and Chung, E., 2019. Light sheet microscopy for histopathology applications. Biomedical engineering letters, pp.1-13.
27. Mahammad, S.N., 2013. SDR based Multi Data Communication System Design. Procedia Engineering, 64, pp.104-114.
28. Poola, P.K., Jayaraman, V., Chaithanya, K., Rao, D. and John, R., 2018. Quantitative label-free technique for morphological evaluation of human sperm—a promising tool in semen evaluation. OSA Continuum, 1(4), pp.1215-1225.
29. PravinR Kshirsagar, Anil N Rakhonde, PranavChippalkatti, " MRI IMAGE BASED BRAIN TUMOR DETECTION USING MACHINE LEARNING", Test Engineering and Management, January- February 2020 ISSN: 0193-4120, Vol. 81, Page No. 3672 – 3680.
30. PravinKshirsagar et.al (2016), "Brain Tumor classification and Detection using Neural Network", DOI: 10.13140/RG.2.2.26169.72805.
31. Pravin R. Kshirsagar, Arpit D. Yadav, Kirti A. Joshi, PranavChippalkatti, Rinali Y. Nerkar (2020) "Classification and Detection of Brain Tumor by using GLCM Texture Feature and ANFIS" Journal of Research in Image and Signal Processing, 5(1), 15- 31 http://doi.org/ 10.5281/zenodo.3732939.